

Earth pressure acting on single driven piles in sand

Poussée des terres agissant sur des pieux isolés battus dans le sable

M. Sabry

Bechtel Power, Frederick, USA

A. Hanna

Department of Building, Civil & Environmental Engineering, Concordia University, Montreal, Canada

ABSTRACT

Earth pressure is playing a paramount role in estimating the capacity of piles driven in sand. In the literature, reports can be found introducing simplifying assumptions to estimate the earth pressure acting on the pile's shaft. Empirical formulas were developed based on limited laboratory or field test data, where high discrepancies were reported.

In this paper, the theory of cavity expansion together with the finite element technique were utilized to develop a numerical model, capable of evaluating the earth pressure acting on the pile's shaft, and accordingly, the corresponding coefficient of passive earth pressure and the overconsolidation ratio in the sand mass.

Analytical model was developed to predict the capacity of these piles, utilizing limit equilibrium method of analysis. It is of interest to note that pile's capacity is significantly influenced by the driven process of the pile, and further the earth pressure acting on the pile's shaft increases due to an increase of the pile's diameter in case of loose or medium sands, while in case of dense sand, the earth pressure decreases due to particle crushing and dilation. Design theory and design procedure are presented for practicing use.

RÉSUMÉ

La poussée des terres joue un rôle primordial dans l'estimation de la capacité portante des pieux battus dans le sable. Dans la littérature, on peut trouver plusieurs articles qui présentent des méthodes d'estimation de la poussée des terres agissant sur un pieu, basées sur des simplifications et des prévisions. En outre, des formules empiriques ont été développées, basées sur des données limitées de laboratoire ou des essais in situ, où des anomalies remarquables ont été notées. Dans cet article, la technique d'expansion de cavité ainsi que la méthode d'élément fini ont été utilisées pour développer un modèle numérique, capable d'évaluer la poussée des terres agissant sur l'axe d'un pieu, et en conséquence, déterminer le coefficient de butée correspondant et le rapport de surconsolidation existant dans un élément de sable adjacent. Un modèle analytique a été développé pour prédire la capacité de ces pieux, en utilisant la méthode d'analyse basée sur l'équilibre limite. Il est important de noter que la capacité portante d'un pieu est considérablement influencée par le processus de battage du pieu. En plus, il a été noté que en cas de sables lâches ou moyennement dense, la poussée des terres agissant sur le pieu augmente en augmentant le diamètre du pieu, alors qu'en cas de sable dense, la poussée des terres diminue due à la dilatation et au écrasement des grains de sable. Un procédé et une théorie de conception sont présentés pour un usage pratique.

Keywords : Single pile, Cohesionless soil, Driven piles, Numerical modelling, Finite Element Technique, Cavity expansion, Earth pressure, overconsolidation ratio, Geotechnical engineering.

1 INTRODUCTION

In the literature, a wide range of discrepancies (+ 900%) can be found among various design theories for predicting the capacity of piles in cohesionless soil (Gavin and Lehane, 1996). It is then recognized that considerable uncertainty remains in the current design theories; perhaps ignoring some viable governing parameters and/or the assumptions used are not realistic (Foray et al, 1998 and Hanna and Nguyen, 2002 and 2003).

Due to the complexity in modelling pile foundations in cohesionless soil, the need for laboratory testing of prototype models arises (Meyerhof, 1976). Experimental investigation on cohesionless soil provides qualitative results and valuable opportunity to observe behaviour. Nevertheless, it does not provide quantitative results due to the difficulties in duplicating field condition in laboratory testing. Accordingly, results may vary with test set-up, sand placing technique, and test procedure. Quite often, experimental data influence researchers during the development of design theories.

The capacity of piles in cohesionless soils is made of two components; the shaft resistance and the tip resistance. These two components depend heavily on the insitu earth pressures after pile installation. Due to the difficulties in evaluating the

existing coefficient of earth pressure, simplifying assumptions were used.

Bolton (1986) studied the effect of sand dilatancy on the shaft resistance and how it affects the angle of shearing resistance of the soil. Hanna and Tan (1973) and Das (1989) examined the shaft resistance in different sand types (loose, medium and dense). Some other researchers presented the factors that affect the shaft resistance; nevertheless they did not incorporate them in a design formula or procedure (Tsien, 1986 Mochtar and Edil, 1988 and Leland, 1991).

2 NUMERICAL MODELLING

An axisymmetric numerical model was developed to simulate the case of a single pile driven in sand during the installation and loading. The model uses the finite element technique together with the theory of cavity expansion.

The size of the mesh used varies with the size of the pile (length and diameter) and the amount of deformation expected during installation and loading. In this investigation, the mesh was taken as 50 times the pile radius in the horizontal direction, and 1.5 times the pile's length in the vertical direction.

The axis of the mesh was taken to coincide with the axis of the pile. The choice of the number of elements and the mesh design reflect a compromise between an acceptable degree of accuracy and computing time. Preliminary tests were performed using a relatively coarser mesh to establish the stress concentrations zones. The results of this stage were used to create a refined mesh, especially, in zones where stresses and deformation expected to change drastically. The nodes along the periphery of the pile as well as those along the vertical boundaries are fixed against displacement in the horizontal direction; yet remain free to move vertically. The nodes constituting the bottom of the mesh were fixed against displacement in both horizontal and vertical directions. Interface elements were installed along the pile's shaft to simulate the friction between the pile and the surrounding sand.

The soil and the pile materials were modelled by 15-noded triangle elements with a quadratic function of displacement. The pile material was assumed to be linear elastic; this is due to the fact that the maximum stresses generated on the pile during installation and loading would not reach the yielding limit of the pile material. The soil was considered to be homogeneous isotropic sand, following the constitutive law of Mohr Coulomb criteria. The range of the pile and the soil parameters used in this investigation are summarized in Table 1 and 2 respectively.

Table 1. Input data for Pile's Material

| Parameter | Value |
|---------------------------------------|-----------------------------------|
| Pile Length | 6 – 15 m |
| Pile Diameter | 0.15 – 0.50 m |
| Young's modulus, E' | 3×10^7 kN/m ² |
| Unit weight, γ | 24 kN/m ³ |
| Poisson's ratio, ν' | 0.1 |
| Interface angle of friction, δ | Variable |

Table 2. Range of parameters of the sand used in the numerical model

| Parameter | Values |
|--|---------------------------------|
| Dry unit weight, γ (kN/m ³) | 17-19 |
| Secant stiffness modulus, E^{ref} (kN/m ²) | $2 \times 10^4 - 6 \times 10^4$ |
| Poisson's ratio, ν_{ur} | 0.3-0.28 |
| Angle of shearing Resistance, ϕ (degrees) | 30 - 40 |

In order to simulate the changes in the earth pressures on the pile's shaft during the installation and the loading processes, the analysis was performed in three stages as demonstrated in Fig. 2. In the first stage, an initial opening of a value of (r_0) was first created in the sand mass; the interface elements were then placed along the opening walls to represent the pile/sand interface. To simulate the insertion of the pile in the sand mass, a prescribed displacement was generated progressively along the pile's perimeter in the axisymmetrical direction. This prescribed displacement (Δr), will, will take place taken place progressively, having a maximum value equal to the pile diameter (D) where:

$$D = 2 \cdot (r_0 + \Delta r) \quad (1)$$

In the second stage, the pile elements were introduced to fill up the produced cavity. This stage represents a transition stage between the pile installation process and the loading process, where the insitu stresses are adjusted due to the presence of the pile and the removal of the prescribed displacement force. In this stage the residual stresses generated during the pile installation were considered as the initial loading condition on the pile and carried over to the loading stage.

In the third stage, axial external load was applied on the pile up to the failure point, and the load-settlement characteristics

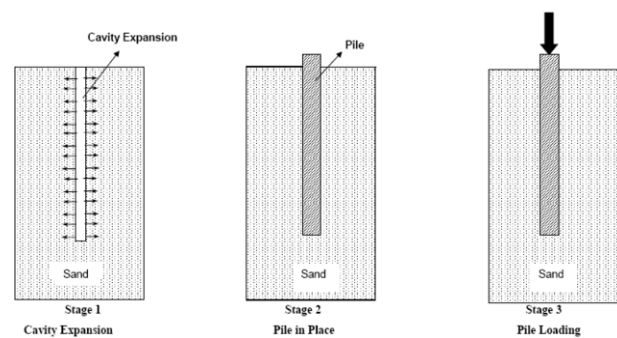


Figure 1. Stages followed in the numerical model.

were recorded. The results produced in the third stage would show the changes in the insitu stresses generated in the soil mass after pile installation up to the failure point.

3 RESULTS

From un-deformed/deformed mesh before/after the cavity expansion. It can be noted that the elements in the horizontal direction were displaced along the pile length as a results of the cavity expansion. The horizontal and vertical stresses in the sand mass shortly after the pile installation increases due to cavity expansion, and accordingly, the earth pressure acting on the pile's shaft, while the vertical stresses did not sensibly increase.

Fig. 2 presents the distribution of the earth pressures on the pile's shaft, in this figure the earth pressure was evaluated as follows:

$$P = K_s \gamma h \quad (2)$$

Where:

K = coefficient of earth pressure

γ = soil effective unit weight

h = the depth from ground surface

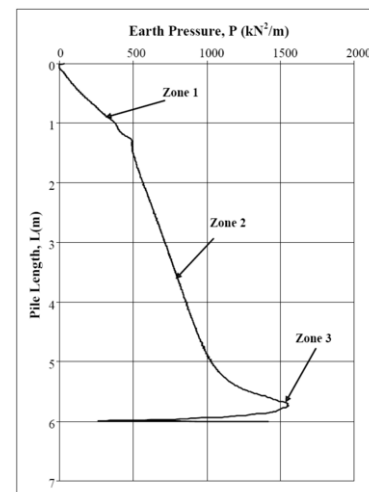


Figure 2. Location of stress zones.

The values of K_s are relatively higher near the pile head, due to the low vertical pressure. Furthermore, K_s decreases with depth up to a certain depth, beyond which K_s increases again near the pile's tip. The increase near the tip is due to the arching effects, which takes place during the pile driving and loading. In addition, the deduced values of K_s are higher than that of the coefficient of passive earth pressure, which is corresponding to the angle of shearing resistance of the sand (ϕ). This increase is mainly due the overconsolidation of the surrounding sand, which takes place during pile installation. The overconsolidation ratio (OCR) was calculated as follows:

$$\text{OCR} \approx (K_s/K_p)^2 \quad (\text{Brooker and Ireland, 1965}) \quad (3)$$

Where:

K_p = Coefficient of passive earth pressure for normally consolidated sand

Furthermore,

$$K_p = \tan(45 + \phi/2)^2$$

The capacity of the pile increases due to an increase of its diameter. It should be made clear herein that pile's diameter contributes to its capacity in three different ways; increasing the pile's shaft, increasing the tip area of the pile and further increasing the earth pressure acting on the pile's shaft due to the increase in the OCR.

The horizontal stresses in the soil mass was significantly increased immediately after the pile installation. This increase is due to the radial compaction, which took place during the cavity expansion. Furthermore, the horizontal stresses decrease directly below the pile's tip up to a level less than the initial value before pile installation. This is due to the tension that took place in the soil mass as a result of the radial displacement. This decrease in the horizontal stress will be eventually diminished during loading and the downward movement of the pile.

The vertical stresses are relatively high near the soil surface due to the heave that occurs on the surface as a result of the lateral displacement of the soil. At the tip level, a sudden reduction in the vertical stress occurs due to the arching effects similar to the horizontal stresses. This reduction in the vertical stress will be eventually reversed due soil compaction, which will take place during loading and the downward movement of the pile's tip.

4 ANALYTICAL MODEL

The deduced stress pattern from the results of the numerical model was idealized as three zones. Fig. 3 presents a schematic sketch of these three zones as follows:

- 1- Zone 1, starts from the pile head and extends slightly below.
- 2- Zone 2, follow zone 1 and covers the mid-section of the pile.
- 3- Zone 3, follow zone 2 and ends at the tip of the pile.

The extent of each zone depends on the pile's diameter, pile's length and the angle of shearing resistance of the sand, ϕ . In this analysis, the horizontal stresses in each zone were evaluated using the coefficient of earth pressure for that zone as deduced from the results of the numerical model. Thus, the shaft resistance can be formulated as follows:

$$Q_s = \sum_{i=1}^3 P_{s_i} \tan \delta \quad (5)$$

Where:

P_{s1} : Total earth pressure in zone 1

P_{s2} : Total earth pressure in zone 2

P_{s3} : Total earth pressure in zone 3

Where

$$P_{s1} = \gamma \pi D \int_0^{L_1} z K_{s1} dz \quad (6)$$

$$P_{s2} = \pi D \int_0^{L_2-L_1} (K_{s2} \cdot \gamma \cdot z + K_{q2} \cdot q_1) dz \quad (7)$$

$$P_{s3} = \pi D \int_0^{L-L_2} (K_{s3} \cdot \gamma \cdot z + K_{q3} \cdot q_2) dz \quad (8)$$

Furthermore:

$$K_{q_i} = \frac{K_{s_i}}{\cos(\beta - \lambda)} \quad (\text{Costet and Sanglerat 1982})$$

β = angle of inclination of the sand surface with the horizontal ($\beta = 0$)

λ = angle of inclination of the pile with the vertical ($\lambda = 0$)

z = distance measured from the ground surface to a given point on the pile's shaft.

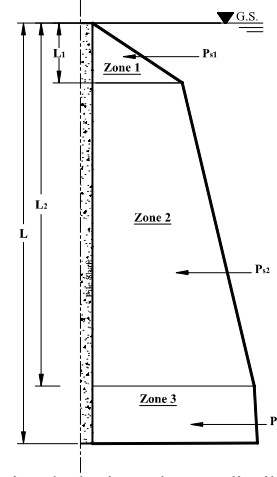


Figure 3. Sketch showing the horizontal stress distribution on the pile's shaft.

Furthermore,

q_1 = surcharge pressure acting on zone 1 ($q_1 = \gamma \cdot L_1$),

q_2 = surcharge pressure acting on zone 2 ($q_1 = \gamma \cdot L_2$)

Based on the results of the numerical model, the following empirical formulae were proposed:

Zone 1:

$$L_1 = \phi(4.3D + 0.65) \quad (\phi \text{ in radians}) \quad (9)$$

$$K_{s1} = 0.6 z e^{5 \tan \phi} + 5 \tan \phi + 6$$

Thus

$$K_{s1} = a_1 \cdot z + b_1 \quad (10)$$

Where:

$$a_1 = 0.6 e^{5 \tan \phi}$$

$$b_1 = 5 \tan \phi + 6$$

Zone 2:

$$L_2 = L - D[(0.02 - 0.1 \tan(\phi))L + 6.5 \tan(\phi) - 1] \quad (11)$$

$$K_{s2} = 250 \tan^4 \phi \left(\frac{D}{z} \right)^{0.7 \tan \phi + 0.02}$$

Thus

$$K_{s2} = a_2 \cdot z^{-b_2} \quad (12)$$

Where:

$$a_2 = 250 \tan^4 \phi (D)^{0.7 \tan \phi + 0.02}$$

$$b_2 = 0.7 \tan \phi + 0.02$$

Zone 3:

$$K_{s3} = \frac{K_{s12} - K_p}{L - L_2} (L - z) + K_p$$

$$K_{s3} = b_3 - a_3 \cdot z \quad (13)$$

Where:

$$a_3 = \frac{K_{s12} - K_p}{L - L_2}$$

$$b_3 = \frac{K_{s12} - K_p}{L - L_2} L + K_p$$

From Eq. (6)

$$P_{s1} = \pi D \gamma \int_0^{L_1} K_{s1} \cdot z \cdot dz = \pi D \gamma \int_0^{L_1} (a_1 z + b_1) z dz$$

Or

$$P_{s1} = \pi D \gamma \left[\frac{a_1}{3} L_1^3 + \frac{b_1}{2} L_1^2 \right] \quad (14)$$

From Eq. (7) and (12)

$$P_{s2} = \pi D \gamma \frac{a_2}{2 - b_2} (L_2^{2-b_2} - L_1^{2-b_2}) \quad (15)$$

From Eq. (8) and (13)

$$P_{s3} = \pi D \gamma \left[\frac{-a_3}{3} (L^3 - L_2^3) + \left(\frac{b_3}{2} \right) (L^2 - L_2^2) \right] \quad (16)$$

Thus the total earth pressure acting on the pile's shaft can be evaluated as follows.

$$P_s = P_{s1} + P_{s2} + P_{s3} \tag{17}$$

Substituting Eqs. (14), (15) and (16) in Eq. (17):

$$P_s = \pi D \gamma \left[\left(\frac{a_1}{3} L_1^3 + \frac{b_1}{2} L_1^2 \right) + \left(\frac{a_2}{2-b_2} (L_2^{2-b_2} - L_1^{2-b_2}) \right) - \left(\frac{a_3}{3} (L^3 - L_2^3) - \frac{b_3}{2} (L^2 - L_2^2) \right) \right] \tag{18}$$

P_s can be also defined as:

$$P_s = \gamma \pi D \int_0^L z K_s dz = \frac{1}{2} \pi D \gamma K_s L^2 \tag{19}$$

Where

K_s = average coefficient of passive earth pressure along the length of the pile,

Equating Eqs. (18) and (17), the average coefficient of earth pressure can be obtained as follows:

$$K_s = \frac{2}{L^2} \left[\left(\frac{a_1}{3} L_1^3 + \frac{b_1}{2} L_1^2 \right) + \left(\frac{a_2}{2-b_2} (L_2^{2-b_2} - L_1^{2-b_2}) \right) - \left(\frac{a_3}{3} (L^3 - L_2^3) - \frac{b_3}{2} (L^2 - L_2^2) \right) \right] \tag{20}$$

Substituting with the value of K_s in Eq. (6), thus:

$$Q_s = \tan \delta \cdot \sum_{i=1}^3 P_{si} = P_s \cdot \tan \delta \tag{21}$$

The values of the average coefficient of earth pressure, K_s determined from Eq. (19) were presented in graphical forms in Figure 17 and accordingly, the shaft resistance, Q_s can be predicted using Eq. (21).

5 COMPARISON WITH FIELD TESTS

The present theories were validated by full-scale pile load tests, which are available in the literature. The measured capacity was compared with the theoretical values predicted by both theories developed in the present investigation; namely zone of influence method and the stress pattern method. The comparisons are presented in Table (3). The discrepancies reported in some tests are due to the presence of ground water and the layered system of the soil strata. Otherwise, a good agreement can be achieved.

From comparing the stress zone method and the zone of influence method with the field tests, it can be noted that the theoretical model based on the zone of influence using the limit equilibrium method provided consistent results, which are

Table 3. Pile load test data description and comparison with the stress pattern theory using (K_s) average.

| ID | Penetration (m) | Diameter (m) | L/D | ϕ (Degrees) | K_s | N° | γ_{sat} (kN/m ³) | Predicted Q_u (kN) | Measured Q_u (kN) | Error (%) |
|----------------------------|-----------------|--------------|--------|------------------|-------|-------------|-------------------------------------|----------------------|---------------------|-----------|
| Visic 1970 (H-15) | 15.00 | 0.46 | 32.82 | 36 | 10 | 26 | 6 | 3325 | 3200 | 3.9 |
| " (H-14) | 11.97 | 0.46 | 26.19 | 39 | 14 | 30 | 6 | 2628 | 2630 | -0.1 |
| " (H-13) | 8.86 | 0.46 | 19.39 | 35 | 11 | 25 | 6 | 1981 | 1872 | 5.8 |
| " (H-12) | 6.13 | 0.46 | 13.40 | 34 | 11 | 23 | 6 | 1450 | 1533 | -5.4 |
| " (H-11) | 3.01 | 0.46 | 6.59 | 31 | 10 | 16 | 8 | 365 | 411 | -11.2 |
| Abe et al (1990) | 16.50 | 0.31 | 54.10 | 25 | 4 | 10 | 11 | 1564 | 1735 | -9.9 |
| Tavenas (J-2) | 8.81 | 0.32 | 27.53 | 34 | 12 | 23 | 9 | 947 | 548 | 72.9 |
| Coyte (1973) | 8.69 | 0.45 | 19.31 | 34 | 10 | 23 | 10 | 2065 | 1496 | 38.0 |
| Webster et al 1994 | 13.80 | 0.61 | 22.62 | 30 | 5 | 16 | 10 | 2674 | 2250 | 21.5 |
| Fellenius (1988) A4 | 37.00 | 0.32 | 114.55 | 32 | 6 | 16 | 5 | 4333 | 2250 | 91.7 |
| G1 | 43.00 | 0.23 | 188.60 | 32 | 6 | 16 | 6 | 5460 | 2536 | 86.0 |
| Mohamad Hussein (2002) | 19.80 | 0.46 | 43.33 | 34 | 7 | 19 | 8 | 8133 | 7340 | 10.8 |
| Beringen et al (1979)1-c | 7.00 | 0.36 | 19.61 | 35 | 14 | 35 | 10 | 2435 | 2440 | -0.2 |
| 2-c | 6.70 | 0.36 | 18.77 | 35 | 14 | 35 | 10 | 2702 | 3000 | -9.9 |
| Gurtowski & Wu (1984) A-c | 29.90 | 0.61 | 49.02 | 25 | 2 | 10 | 8 | 4277 | 4626 | -7.5 |
| B-c | 25.60 | 0.61 | 41.97 | 25 | 2 | 10 | 11 | 4547 | 4793 | -5.1 |
| Mansour & Kaufman (1956) 4 | 20.12 | 0.43 | 46.79 | 28 | 4 | 10 | 8 | 3440 | 3540 | -2.8 |
| 5 | 13.70 | 0.43 | 31.64 | 25 | 3 | 10 | 8 | 1528 | 1470 | 3.9 |
| 6 | 19.80 | 0.48 | 41.08 | 25 | 3 | 10 | 8 | 3304 | 3470 | -4.8 |
| 7 | 19.80 | 0.46 | 43.33 | 28 | 4 | 14 | 9 | 3246 | 3109 | 4.4 |
| Mey et al. (1985) | 18.00 | 0.91 | 19.69 | 27 | 3 | 13 | 10 | 5380 | 5080 | 5.9 |

higher than the field results. This is due to assumption of general mechanism acting on the pile without considering the local changes in the stresses acting on the pile's shaft. This is due to the fact that limit equilibrium method, which was widely used in literature, did not take into account the driving effect on pile capacity. Furthermore, the comparison, which was based on the stress pattern method revealed good agreement.

6 CONCLUSION

A static numerical model was developed to simulate the effects of pile installation and pile's diameter on the passive earth pressure acting on the pile's shaft. The effect of pile installation on the values of the coefficients of passive earth pressure and the overconsolidated ratio were examined. The model developed utilizes the theory of cavity expansion and the finite element technique. The following can be concluded:

Due to pile installation, the horizontal stresses acting on the pile's shaft increase while the vertical stresses remained unchanged, which leads to an increase in the coefficients of passive earth pressure and accordingly to the OCR ratio.

Due to pile installation, dilation of the surrounding soil will take place in the shallow depths leading to a reduction in the vertical stresses in this zone and significant increase in the passive earth pressure. While at deeper depths, close to the tip, the horizontal stresses increases rapidly due to the high confining pressure in this zone. Immediately below the pile's tip arching takes place and accordingly the passive earth pressure reduces.

The pile diameter was found to contribute to the value of the coefficient of earth pressure which was solely evaluated based on the angle of shearing resistance of sand.

By comparing the theories developed with the available field data, it was concluded that the theory of the stress pattern gives good agreement with the field results.

ACKNOWLEDGMENT

The financial supports received from the Natural Science and Engineering Research Council of Canada (NSERC) and Concordia University are acknowledged.

REFERENCES

Alsiny, A., Vardoulakis, I. and Drescher, A. (1992), "Deformation Localization in Cavity Inflation Experiments on dry sand", *Geotechnique*, v 44, n 2, pp 365-366.

Foray, B., Balachowski, L. and Colliat, J-L. (1998), "Bearing Capacity of Model piles Driven into dense Overconsolidated Sand," *Canadian Geotechnical Journal*, 35, pp(374-385).

Hanna, A. M. and Nguyen, T. Q. (2002), "An Axisymmetric Model for Ultimate Capacity of a single Pie in Sand", *Soils and Foundation*, Vol.42, No.2, pp 47-58.

Hanna, A.M. and Nguyen, T.Q. 2003. "Shaft resistance of Single Vertical and Batter Piles in Sand Subjected to Axial Compression Loading. *ASCE, Journal of Geotechnical and Environmental Engineering*. 129 (3).

Mabsout, Mounir E., Sadek, Salah and Smayra, Toufic E. (1999), "Pile Driving By Numerical Cavity Expansion", *Int. J. Numer. Anal. Meth. Geomech.*, 23, pp 1121-1140.

Meyerhof G. G. (1976), "Bearing Capacity and Settlement of pile foundations", *The Eleven Terzaghi Lecture, J. Geotech. Div. Am. Soc. Civ Engrs* v102 pp. 195-228.

Vesic, A. S. (1972), "Expansion of Cavities in Infinite Soil Mass", *J. Geotech. Engrg.*, ASCE, 98(3), pp 265-290.